19th IMEKO TC 4 Symposium and 17th IWADC Workshop
Advances in Instrumentation and Sensors Interoperability
July 18-19, 2013, Barcelona, Spain

Modeling Sine-Wave Image Component Contribution to Discrete Spectrum

Daniel Belega[1], Dominique Dallet[2], Dario Petri[3]

[1] *Department of Measurements and Optical Electronics, University Politehnica of Timisoara, Bv. V. Parvan, Nr. 2, 300223, Timisoara, Romania, e-mail*: *daniel.belega@etc.upt.ro*
[2] *IMS Laboratory, University of Bordeaux-IPB ENSEIRB MATMECA, 351 Cours de la Libération, Bâtiment A31, 33405, Talence Cedex, France, e-mail: dominique.dallet@ims-bordeaux.fr*
[3] *Department of Industrial Engineering, University of Trento, 38123, Trento, Italy, e-mail: dario.petri@unitn.it*

Abstract **-** In this paper the analytical expression of the contribution of the fundamental image component to the discrete spectrum of a sine-wave weighted by a cosine class window is derived. It is then analysed for some commonly used windows in the case when the considered Discrete Fourier Transform (DFT) samples fall either inside or outside the band defined by the window spectrum main lobe centred at the sine-wave fundamental frequency. From the achieved results some conclusions about the behaviour of the image component contribution to the discrete spectrum of a sine-wave are drawn. The accuracies of the derived expressions are verified through computer simulations.

I. Introduction

Sine-waves are often used in engineering applications since they can be generated easily with a specified accuracy and are simple to handle theoretically. To estimate the parameters of a sine-wave corrupted by a small amount of noise, as often occur in many applications fields such as in instrumentation and measurements, Discrete Fourier Transform (DFT)-based methods are preferred since they provide enough accurate estimates, exhibit a low computational effort, and are easy to implement [1]-[6]. Indeed, a simple post-processing of discrete spectrum samples close to the sine-wave frequency allows to achieve accurate parameter estimates. Unfortunately, estimation accuracy is affected by both spectral leakage due to the finite duration observation interval [7] and picket-fence effect due to granularity between adjacent DFT samples [5]. Both these detrimental effects can be removed by windowing the discrete-time sine-wave [8] and applying the so-called Interpolated DFT (IpDFT) method [4]-[6]. However, spectral interference from the sine-wave image component can significantly affect estimation accuracy, particularly when the number of acquired sine-wave cycles is small. Computer simulations showed that the contribution of the image interference to discrete spectrum samples close to the sine-wave fundamental frequency has a sinusoidal behaviour [9], [10]. However, its analytical expression has not yet published in the scientific literature. This paper is aimed at filling this gap in the case when the analysed discrete-time sine-wave is weighted by a cosine class window [11]. The derived expression is analysed for some commonly used windows when the considered DFT samples fall either inside or outside the band defined by the window spectrum main lobe centred at the sine-wave fundamental frequency. The accuracies of the derived expressions are verified by means of computer simulations.

II. Analytical expression of the contribution from the spectral interference

Let us consider a discrete-time sine-wave $x(m)$ with frequency f, amplitude A, and initial phase ϕ, achieved from a continuous-time sine-wave sampled at frequency f_s, i.e.:

$$x(m) = A\sin(2\pi fm + \phi), \qquad m = 0,1,2,\ldots \tag{1}$$

The frequency f represents the ratio between the continuous-time sine-wave frequency f_x and the sampling frequency f_s. It is assumed that $f_x < 0.5f_s$ to satisfy the Nyquist theorem. When M samples are acquired we have:

$$f = \frac{f_x}{f_s} = \frac{\nu}{M} = \frac{l+\delta}{M}, \tag{2}$$

where l and δ ($-0.5 \le \delta < 0.5$) are the integer and the fractional parts of the number of acquired sine-wave cycles ν, respectively. The sampling process can be either coherent ($\delta = 0$) or non-coherent ($\delta \neq 0$). The latter case is often encountered in practice due to the lack of synchronization between the sine-wave and sampling frequencies. To reduce spectral leakage caused by the finite length of the observation interval, the acquired

samples are weighted by a suitable window $w(\cdot)$, so obtaining the signal $x_w(m) = x(m)\cdot w(m)$, $m = 0, 1,\ldots, M-1$. A cosine class window is often employed [11], i.e.:

$$w(m) = \sum_{h=0}^{H-1} (-1)^h a_h \cos\left(2\pi h \frac{m}{M}\right), \quad m = 0,1,\ldots,M-1 \tag{3}$$

where a_h, $h = 0, 1,\ldots, H-1$, are the windows' coefficients and H is the number of window terms.
The DFT of the windowed signal $x_w(\cdot)$ can be expressed as [1], [6]:

$$X_w(k) = \frac{A}{2j}\left[W(k-l-\delta)e^{j\phi} - W(k+l+\delta)e^{-j\phi}\right], \qquad k = 0,1,\ldots,M-1 \tag{4}$$

where $W(\cdot)$ is the Discrete Time Fourier Transform (DTFT) of the window $w(\cdot)$, given by [3]:

$$W(\lambda) \cong \frac{M\lambda\sin(\pi\lambda)}{\pi} e^{-j\pi\lambda} \sum_{h=0}^{H-1} \frac{(-1)^h 0.5 a_h}{\lambda^2 - h^2} = \frac{M\lambda\sin(\pi\lambda)}{\pi} e^{-j\pi\lambda} W_0(\lambda), \qquad \text{if} \quad |\lambda| << M \tag{5}$$

in which $W_0(\cdot)$ is implicitly defined by the equation.
It should be noted that the last term in (4) represents the contribution from the image component.
In particular, the DFT samples $|X_w(l+n)|$ can be expressed as (see (A.9) in the Appendix):

$$|X_w(l+n)| \cong \frac{A}{2}|W(n-\delta)| + \frac{A}{2} s_n \cos(2\pi\delta + 2\phi)|W(2l+n+\delta)|, \qquad \text{if} \quad |n| << M \tag{6}$$

where $s_n = \text{sgn}[(n-\delta)W_0(n-\delta)W_0(n+2l+\delta)]$, in which the function sgn(·) is the sign function. Expression (6) shows that the contribution due to the image component is:

$$\varepsilon_n(l,\delta) = |X_w(l+n)| - \frac{A}{2}|W(n-\delta)| \cong \frac{A}{2} s_n \cos(2\pi\delta + 2\phi)|W(2l+n+\delta)|, \quad \text{if} \quad |n| << M \tag{7}$$

that is, a cosine function with argument 2ϕ and amplitude equal to $0.5A|W(n+2l+\delta)|$.

III. Behaviour of the contribution from the spectral interference

The aim of this section is to analyse as the behaviour of the contribution (7) depends on the distance between the sine-wave frequency and the frequency of the considered DFT sample. Commonly used cosine class windows are considered, i.e. [11]:

- two-, three-, and four-term Minimum Sidelobe Level (MSL) windows;
- three- and four-term Rapid Sidelobe Decay with Minimum Sidelobe Level (RSD-MSL) windows;
- two-, three-, and four-term Maximum Sidelobe Decay (MSD) windows.

Spectrum samples close to the sine-wave frequency, that is corresponding to $|n| \le H-1$ in (7), are often used to estimate the sine-wave parameters [1] - [6]. Computer simulations performed for different values of the integer and the fractional parts l and δ of the number of acquired sine-wave cycles showed that the term s_n in (7) is given by:

$$s_n = (-1)^{n+1}\,\text{sgn}(\delta), \quad \text{if} \quad |n| \le H-1 \tag{8}$$

when the MSL windows are adopted,

$$s_n = (-1)^{n+H-1}\,\text{sgn}(\delta), \quad \text{if} \quad |n| \le H-1 \tag{9}$$

when the RSD-MSL windows are adopted, and

$$s_n = (-1)^{n+H}\,\text{sgn}(\delta), \quad \text{if} \quad |n| \le H-1 \tag{10}$$

when the MSD windows are adopted. Thus, when $|n| \le H-1$, the contributions from the image component exhibit opposite signs in subsequent DFT samples. This behaviour has been already reported in the literature, but just in the case of MSD windows [9], [10].
Fig. 1 shows the image component contribution $\varepsilon_n(l,\delta)$ returned by both (7) and simulations as a function of the sine-wave phase ϕ when the two-term (Fig. 1(a)) and the three-term (Fig. 1(b)) MSL windows, the three-term

(Fig. 1(c)) and the four-term (Fig. 1(d)) RSD-MSL windows, the two-term (Fig1(e)), and the three-term (Fig. 1(f)) MSD windows are considered. The terms s_n are returned by (8), (9), and (10), respectively. When the two-term MSD or MSL windows are adopted, the values of n were equal to −1, 0, and 1, whereas when the three-term MSD or MSL windows, and the RSD-MSL windows are adopted, these are n = –2, –1, 0. The reported results were achieved by choosing: A = 1, ν = 7.2 (l = 7, δ = 0.2), M = 4096. The phase ϕ was varied in the range [0, 2π) with a step of π/50 rad.

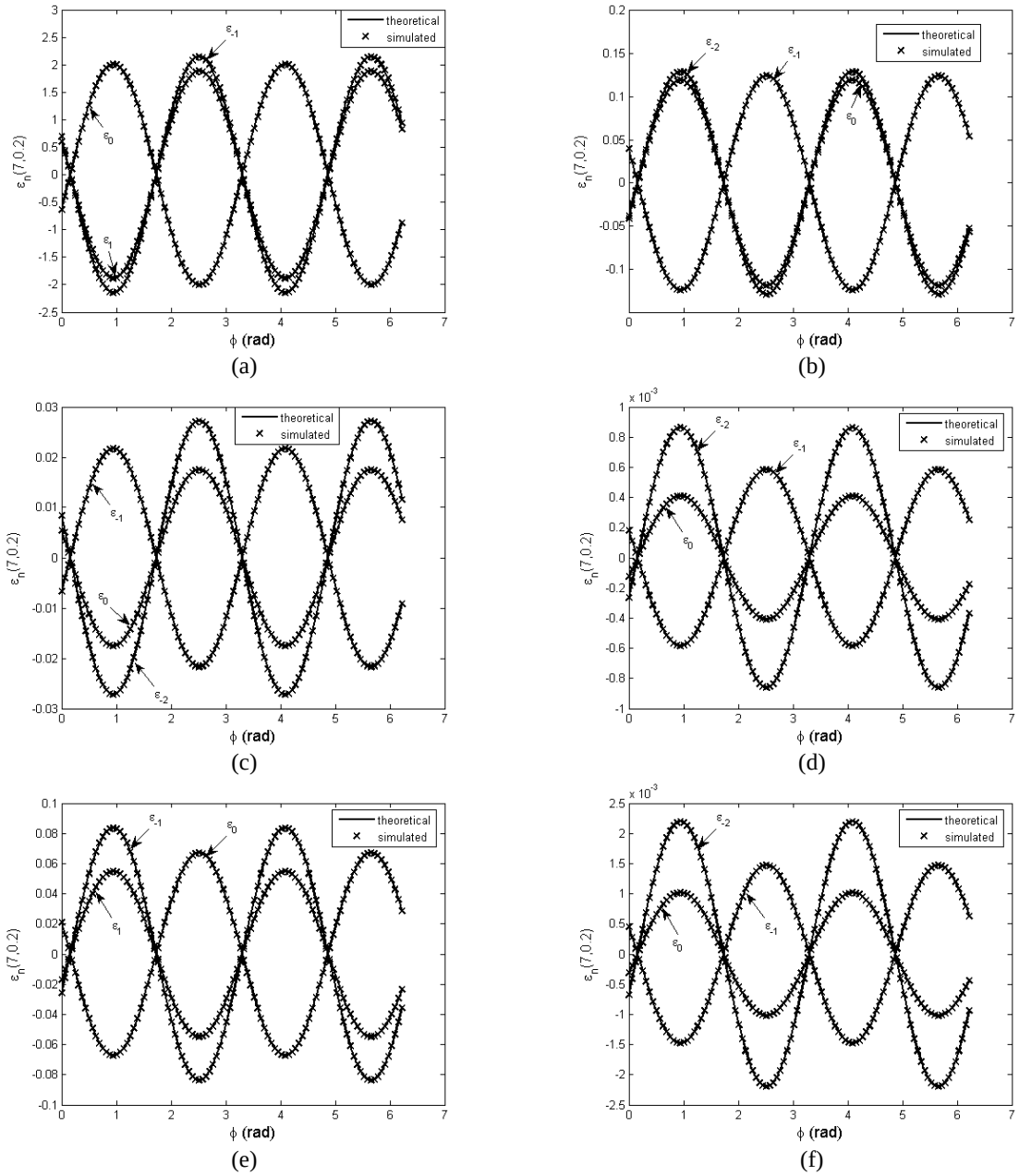

Fig.1. Image component contribution $\varepsilon_n(7, 0.2)$ returned by equation (7) ('continuous line') and computer simulations ('crosses') versus sine-wave phase ϕ: (a) two-term MSL window; (b) three-term MSL window; (c) three-term RSD-MSL window; (d) four-term RSD-MSL window; (e) two-term MSD window; (f) three-term MSD window; n = –1, 0, 1, for two-term windows and n = –2, -1, 0, for three-term windows. Sine-wave amplitude A = 1 and number of analysed samples M = 4096.

As shown by Fig. 1 the agreement between theoretical and simulation results is very good.
Conversely, when $|n| \geq H$, the image component contributions do not exhibit opposite signs in subsequent DFT

samples. For example, the contributions from the image component $\varepsilon_n(7, 0.2)$ returned by (7) and simulation results for $n = H$, $H + 1$, and $H + 2$ are shown in Fig. 2 as a function of the sine-wave phase ϕ when the four-term RSD-MSL (Fig. 2(a)) and the three-term MSD (Fig. 2(b)) windows are adopted. The same simulation parameters used in Fig. 1 were considered.

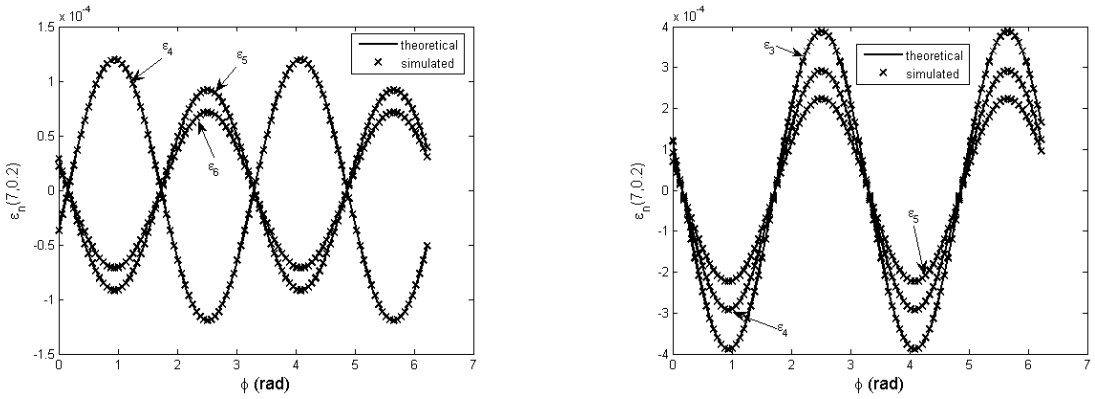

(a) (b)

Fig.2. Image component contribution $\varepsilon_n(7, 0.2)$ returned by equation (7) ('continuous line') and computer simulations ('crosses') versus sine-wave phase ϕ: (a) four-term RSD-MSL window and $n = 4,\ 5,\ 6$; (b) three-term MSD window and $n = 3,\ 4,\ 5$. Sine-wave amplitude $A = 1$ and number of analysed samples $M = 4096$.

For the considered windows, Fig. 2 shows that the agreement between theoretical and simulation results is very good. In the case of the four-term RSD-MSL window (Fig. 2(a)), both s_5 and s_6 are equal to 1 and the image component contributions to the DFT samples $|X_w(l + 5)|$ and $|X_w(l + 6)|$ do not exhibit opposite signs. The same occurs in the case of the three-term MSD window (Fig. 2(b)) for the DFT samples $|X_w(l + 4)|$, $|X_w(l + 5)|$, and $|X_w(l + 6)|$. It should also be noticed that, when considering DFT samples falling outside the band defined by the window spectrum main lobe centred at the sine-wave frequency, the accuracy of (7) is somewhat worse for the MSL windows than the MSD and RSD-MSL windows. This occurs because the accuracy of (7) for small values of $|n|$ depends on the level of the window sidelobes close to $M/2$, which is higher for the MSL windows when M is enough high.

IV. Conclusions

This paper has been aimed at deriving the analytical expression of the contribution of the fundamental image component to the discrete spectrum of a sine-wave weighted by a cosine class window. The derived expression has been analysed for the two-, three-, and four-term MSL and MSD windows and the three- and the four-term RSD-MSL windows. It has been shown that the contributions from the image component exhibit opposite signs in subsequent DFT samples for the $(2H - 1)$ DFT samples falling inside the band defined by the window spectrum main lobe centred at the sine-wave frequency. A different behaviour occurs for DFT samples falling outside that band. The accuracies of the derived expressions have been confirmed through computer simulations.

APPENDIX
Analytical expression of the DFT samples $|X_w(l + n)|$

Using the identity $|z_1 + z_2|^2 = |z_1|^2 + |z_2|^2 + 2\,\mathrm{Re}\{z_1 z_2^*\}$, where z_1 and z_2 are complex-valued variables, $\mathrm{Re}\{\cdot\}$ represents the real part of its argument and * denotes the conjugation operator, from (4) it follows that:

$$|X_w(l+n)|^2 = \frac{A^2}{4}\left[|W(n-\delta)|^2 + |W(2l+n+\delta)|^2 - 2\,\mathrm{Re}\{W(n-\delta)W^*(2l+n+\delta)e^{j2\phi}\}\right], \quad |n| << M \tag{A.1}$$

The last term in the square brackets of (A.1) can be expressed as:

$$\begin{aligned}\mathrm{Re}\{W(n-\delta)W^*(2l+n+\delta)e^{j2\phi}\} = \\ [\mathrm{Re}\{W(n-\delta)\}\mathrm{Re}\{W(2l+n+\delta)\} + \mathrm{Im}\{W(n-\delta)\}\mathrm{Im}\{W(2l+n+\delta)\}]\cos(2\phi) \\ + [\mathrm{Re}\{W(n-\delta)\}\mathrm{Im}\{W(2l+n+\delta)\} - \mathrm{Im}\{W(n-\delta)\}\mathrm{Re}\{W(2l+n+\delta)\}]\sin(2\phi).\end{aligned} \tag{A.2}$$

ISBN-10: 84-616-5438-2 | ISBN-13: 978-84-616-5438-3

where Im{·} represents the imaginary part of its argument.
Using (5) it can be shown that:

$$\mathrm{Re}\{W(n-\delta)\} = -\mathrm{sgn}[(n-\delta)\delta W_0(n-\delta)]\cos(\pi\delta)|W(n-\delta)| \tag{A.3}$$

$$\mathrm{Im}\{W(n-\delta)\} = -\mathrm{sgn}[(n-\delta)\delta W_0(n-\delta)]\sin(\pi\delta)|W(n-\delta)| \tag{A.4}$$

$$\mathrm{Re}\{W(2l+n+\delta)\} = \mathrm{sgn}[\delta W_0(2l+n+\delta)]\cos(\pi\delta)|W(2l+n+\delta)|, \tag{A.5}$$

$$\mathrm{Im}\{W(2l+n+\delta)\} = -\mathrm{sgn}[\delta W_0(2l+n+\delta)]\sin(\pi\delta)|W(2l+n+\delta)|, \tag{A.6}$$

where sgn(·) represents the sign function.
By replacing (A.3) – (A.6) in (A.2) it follows:

$$\begin{aligned}&\mathrm{Re}\{W(n-\delta)W^*(2l+n+\delta)e^{j2\phi}\}\\ &\quad= -\mathrm{sgn}[(n-\delta)W_0(n-\delta)W_0(2l+n+\delta)]\cos(2\pi\delta+2\phi)|W(n-\delta)||W(2l+n+\delta)|\\ &\quad= -s_n\cos(2\pi\delta+2\phi)|W(n-\delta)||W(2l+n+\delta)|,\end{aligned} \tag{A.7}$$

where $s_n = \mathrm{sgn}[(n-\delta)W_0(n-\delta)W_0(2l+n+\delta)]$.
By replacing the above expression in (A.1) we obtain:

$$|X_w(l+n)|^2 = \frac{A^2}{4}\left[|W(n-\delta)|^2 + |W(2l+n+\delta)|^2 + 2s_n\cos(2\pi\delta+2\phi)|W(n-\delta)||W(2l+n+\delta)|\right] \tag{A.8}$$

Since $|W(n-\delta)| >> |W(2l+n+\delta)|$ and considering the first-order Taylor's series expansion of $(1+x)^{1/2}$ we finally achieve:

$$|X_w(l+n)| \cong \frac{A}{2}|W(n-\delta)| + \frac{A}{2}s_n\cos(2\pi\delta+2\phi)|W(2l+n+\delta)|, \qquad |n| << M \tag{A.9}$$

References

[1] C. Offelli and D. Petri, "A frequency-domain procedure for accurate real-time signal parameter measurement", *IEEE Trans. Instrum. Meas.*, vol. 39, no. 2, pp. 363-368, Apr. 1990.
[2] M. Novotný, D. Slepička, and M. Sedláček, "Uncertainty analysis of the RMS value and phase in frequency domain by noncoherent sampling", *IEEE Trans. Instrum. Meas.*, vol. 56, no. 3, pp. 983-989, Jun. 2007.
[3] D. Belega, D. Dallet, and D. Petri, "Accuracy of the normalized frequency estimation of a discrete-time sine-wave by the energy-based method", *IEEE Trans. Instrum. Meas*., vol. 61, no. 1, pp. 111-121, Jan. 2012.
[4] D. C. Rife and G. A. Vincent, "Use of the discrete Fourier transform in the measurement of frequencies and levels of tones", *Bell Syst. Tech. J.*, vol. 49, pp. 197-228, 1970.
[5] C. Offelli and D. Petri, "Interpolation techniques for real-time multifrequency waveform analysis", *IEEE Trans. Instrum. Meas.*, vol. 39, no. 1, pp. 106-111, Feb. 1990.
[6] D. Belega and D. Dallet, "Multifrequency signal analysis by interpolated DFT method with maximum sidelobe decay windows", *Measurement*, vol. 42, no. 3, pp. 420-426, Apr. 2009.
[7] A. Ferrero and R. Ottoboni, "High-accuracy Fourier analysis based on synchronous sampling techniques", *IEEE Trans. Instrum. Meas.*, vol. 41, no. 6, pp. 780-785, Dec. 1992.
[8] F. J. Harris, "On the use of windows for harmonic analysis with the discrete Fourier transform", *Proc. of the IEEE*, vol. 66, no. 1, pp. 51-83, Jan. 1978.
[9] D. Agrež, "Weighted multipoint interpolated DFT to improve amplitude estimation of multifrequency signal", *IEEE Trans. Instrum. Meas.*, vol. 51, no. 2, pp. 287-292, Apr. 2002.
[10] D. Belega, D. Dallet, and D. Petri, "Statistical description of the sine-wave frequency estimator provided by the interpolated DFT method", *Measurement*, vol. 45, no. 1, pp. 109-117, Jan. 2012.
[11] A. H. Nutall, "Some windows with very good sidelobe behaviour", *IEEE Trans. Acoust., Speech, Signal Proces.*, vol. ASSP-29, no. 1, pp. 84-91, Feb. 1981.